International Journal of Chemical and Biochemical Sciences
(ISSN 2226-9614)

Journal Home page: www.iscientific.org/Journal.html

The Study of Zinc Oxide Nanowires Properties Prepared by Modified Microwave-Assisted Sonochemical Deposition Method at Different Solution Concentrations

Maryam Mohammad[1,2,3], Mohd Firdaus Malek[1,2]*, Muhammad Faizal Abd Halim[1], Kelvin Alvin Eswar [1,2,4], Rabiatuladawiyah Md Akhir[1,2], Najwa Ezira Ahmed Azhar [1,5], Nurfazianawatie Mohd Zin [1,2], Mohamad Hafiz Mamat[5], Zuraida Khusaimi[1,2], Noor Asnida Asli[1,2], Mohd Husairi Fadzilah Suhaimi[1,2] and Mohamad Rusop Mahmood[1,5]

[1]NANO-SciTech Lab (NST), Centre for Functional Materials and Nanotechnology (FMN), Institute of Science (IOS), Universiti Teknologi MARA (UiTM), 40450 Shah Alam, Selangor, Malaysia.

[2]School of Physics and Materials Studies, Faculty of Applied Sciences, Universiti Teknologi MARA (UiTM), 40450 Shah Alam, Selangor, Malaysia.

[3]School of Physics and Materials Studies, Faculty of Applied Sciences, Universiti Teknologi MARA (UiTM) Perak Branch, Tapah Campus, 35400 Tapah Road, Perak, Malaysia.

[4]School of Physics and Materials Studies, Faculty of Applied Sciences, Universiti Teknologi MARA (UiTM) Sabah Branch, Tawau Campus, 91032 Tawau, Sabah, Malaysia.

[5]NANO-ElecTronic Centre (NET), School of Electrical Engineering, College of Engineering, Universiti Teknologi MARA (UiTM), 40450 Shah Alam, Selangor, Malaysia.

Abstract

Zinc oxide nanowires (ZnO NWs) have been successfully synthesized via a modified microwave-assisted sonochemical deposition (MMASD) method using zinc acetate dehydrate as the starting material with varying deposition solution concentrations of 6.25, 12.5, 25, 50, and 75 mM. The deposition time was optimized at 60 minutes deposited at a microwave power of 600 Watts and the effect of molarity on the morphological, structural, and optical properties of the ZnO NWs was investigated where the samples were characterized by field emission scanning electron microscope (FESEM), X-ray diffraction (XRD), and ultraviolet-visible spectroscopy (UV-Vis). Morphological properties obtained showcase hexagonal wurtzite nanostructures of ZnO with varying diameter sizes dependent on the deposition solution concentration. The XRD spectra also showed that the ZnO NWs produced are highly crystalline, exhibiting sharper and narrower intensity of (002) peaks as the molarity of the deposition solution increases. The transmittance spectra obtained by UV-Vis are highest at 12.5 mM and decreases at higher concentration.

Keywords: Zinc oxide, Nanowires, Molarity, Concentration, Sonochemical, Microwave-assisted

Full length article **Corresponding Author*, e-mail: mfmalek07@uitm.edu.my; mfmalek07@gmail.com

1. Introduction

Since it possesses unique characteristics including a broad direct bandgap (3.37 eV) and substantial exciton-

binding energy (60 meV), zinc oxide (ZnO) has received a lot of interest and has been studied for decades [1-2]. Furthermore, ZnO is a substance that is non-toxic, chemically stable, and reasonably priced. This material's advantages have reportedly been claimed to improve the functionality of sensors, photocatalysis, optoelectronic devices, and many other applications [3-5]. Amid plentiful procedures to synthesize this material, the solution-based synthesis approach is the most widely used method to produce a wide range of 1D nanometer to micrometer of ZnO NSs.

These NSs include rods, plates, tubes, rings, tetrapods, prisms, pyramids, spheres, hollow structures, flower-like, and multi needle-shaped crystals [6-8]. Amongst these structures however, ZnO nanowires (ZnO NWs) were particularly notable due to their quasi-one-dimensional (1-D) architectures displaying quantum confinement phenomena and huge surface-to-volume ratios. It may be described as a 1-D channel with electron, hole, and photon absorption, emission, and transport, resulting in significant confinement effects on carriers and photons and a variety of unique optical and electrical features for device applications [9-11]. Besides that, one-dimensional nanostructures (NSs), such as nanowires grown on a substrate, have a higher surface-to-volume ratio than nanoparticles (NPs) deposited on a flat surface, resulting in increased photocatalytic activity via enhanced adsorption of target organic molecules onto the catalyst surface [12]. Additional advantages include a wide range of substrate materials and geometries, as well as a simple crystal-growth technique that enables far lower manufacturing costs than other semiconductors used in nanotechnology [13-14].

The creation of nanowires was also specifically targeted owing to its hexagonal wurtzite structure of ZnO, which is the most thermodynamically stable and hence most prevalent of the three forms, namely wurtzite, zinc-blende, and rock salt [15-16]. Various research has been carried out in order to regulate the formation of ZnO nanowires for specific purposes by varying the synthesis method, reactant, and parameter [17-18]. However, the traditional method of producing ZnO NWs by solution-based approach focused more on the effects of stabilizer instead of reactant dispersion which caused a non-homogeneous reaction during the mixing process of precursor and solvent will contribute to the formation of a large particle size and reduced the surface area of the nanostructures. This behavior will result in low electron transit and significant recombination across defective states such as grain boundaries [19]. In addition, despite the fact that the common growth techniques for ZnO NWs currently used are largely successful, including chemical and physical methods like thermal evaporation, chemical vapor deposition (CVD), and cyclic feeding CVD, sol-gel deposition, electrochemical deposition, hydrothermal and solvothermal growth, as well as surfactant and capping agents-assisted growth [20-29]. They do have certain disadvantages, such as low productivity or severe impurities from their employed aid ie. Catalyst or precursor, which can pose real issues for their nanodevice applications [30].

The other limitation would be that these technologies require severe conditions, such as high heat and pressure, expensive materials, and time-consuming procedures. In more recent studies, the introduction of microwave-assisted methods has been proven to help overcome these problems due to their excellent mechanism in helping to expedite the synthesis process while significantly improving the ZnO properties [31-33]. Scalability, low energy consumption, quick expansion, low cost, and simplicity of handling are only a few of the benefits that microwave technology itself offers, making it a highly praised method to deal with these typical problems [34-36]. Additionally, compared to a more typical method of ZnO NS synthesis, the microwave-assisted method provides higher control over the structure and dimensional dispersion of ZnO NSs which results in consistency of the experimentation outcome [37]. Additionally, microwave irradiation is essential for chemical processes that take place in aqueous media, decreases the amount of production time and cost, reducing the particle size with a narrow size distribution, increasing the product yield rate, and generating high-purity products in comparison to conventional methods [38-43]. Hence, we proposed our very own novel modified microwave-assisted sonochemical deposition method as an excellent alternative to the conventional method where the difference is with the incorporation of a very effective and often employed solution-based (sonochemical) technique whereby the sonification was incorporated during the mixing process, to significantly improve the interaction between the precursor and stabilizing agent and thus provide better overall control of the features of the nanostructure. It will then be further assisted by microwave irradiation to expedite the production process while also studying the effect of the different molar concentrations of the deposition solution on the properties of ZnO NWs produced.

2. Materials and Methods

The research methodology comprises of three different phases as summarized. The first process would be the preparation and cleaning of the glass substrates. Then the preparation of ZnO NPs thin film using ultrasonic-assisted sol-gel spin coating technique producing ZnO NPs array. It will then undergo a deposition process in the microwave to produce ZnO NWs. Analysis of data was done to investigate the morphological structures of the samples by using Field Emission Scanning Electron Microscope (FESEM, JEOL JSM-7600F), X-ray Diffraction (XRD) (XRD, PANalytical X'Pert PRO), and Ultraviolet-visible (UV-Vis) spectrometer (Cary 5000).

2.1. Preparation of ZnO nanoparticles seeded layer thin films

Zinc Oxide-Based Nanoparticles were prepared as a seed layer of thin films on a glass substrate which was deposited by an optimized ultrasonic-assisted sol-gel (sonochemical) spin-coating technique [44-45]. The sonicated sol–gel ZnO was prepared by dissolving 0.4 M zinc acetate dehydrates [Zn $(CH_3COO)_2 \cdot 2H_2O$; Merck; 98%] which acts as the precursor in the solvent of 2-methoxy ethanol [$C_3H_8O_2$; Merck] at room temperature. Then, 1 at% of aluminum nitrate nonahydrate [Al $(NO_3)_3.9H_2O$; Analar] and 0.4 monoethanolamines [MEA, C_2H_7NO; R&M] were added into the solution as dopant and stabilizer respectively. The molar ratio of MEA to zinc acetate dehydrate was maintained at 1:1, and the resultant solution was stirred at 80 ºC for 40 minutes to yield a clear and homogeneous solution. Afterward, the solution was sonicated at 50ºC for 30 minutes using an ultrasonic water bath (Hwasin Technology Powersonic 405, 40kHz) and

cooled to room temperature. The solution will then be used to coat the glass substrate using the spin coating technique where 10 drops of the solution are deposited onto the substrate at a speed of 3000 rpm for 30 s. Lastly, the samples were preheated in an atmosphere ambient at 300℃ for 10 minutes to remove solvent.

The deposition processes were repeated for the second to the fifth layer of film to achieve the required film thickness. All samples were annealed in a furnace at a temperature of 500 ℃ for 1 hour.

2.2. Deposition of ZnO nanostructures via a microwave-assisted sonochemical technique

ZnO NWs were grown via the novel MMASD method. 6.25, 12.5, 25, 50, and 75 m M concentration of the solution was prepared using Zinc acetate dehydrate [(Zn $(CH_3COO)_2{\cdot}2H_2O$; Merck] and 0.01M hexamethylenetetramine [HMTA, $C_6H_{12}N_4$; Merck] as a precursor and stabilizer, respectively [46]. The reagents were dissolved and reacted in a beaker filled with 1000 mL distilled water as a solvent and stirred at 80 ºC for 30 minutes to yield a clear and homogeneous solution. Next, the solution was sonicated at 50 ºC for 30 minutes using an ultrasonic water bath (Hwasin Technology Powersonic 405, 40 kHz). The solution was then aged at room temperature for 1 hour and poured into a Schott bottle of 250 ml volume capacities where the optimized seed layer-coated glass substrates were placed at the bottom of the container. Afterward, the container was placed inside the 2.45 GHz microwave (SHARP 25L Microwave Oven R352ZS) which was set to a microwave power of 600 Watt for 60 minutes. Once done, the samples were annealed at a temperature of 500 ℃ for 1 hour. The procedures described above are depicted in **Figure 1**.

2.3. Characterization method

The structural and morphological properties were characterized by X-ray diffraction (XRD, PANalytical X'Pert PRO) with Cu K-alpha radiation of a wavelength of 1.54 Å and field emission scanning electron microscope (FESEM, JEOL JSM-7600F). The optical properties were characterized by UV-visible spectroscopy (UV-Vis, Cary 5000).

3. Results and discussions

3.1. Morphological and structural study

Figure 2 (a) to (e) shows the top image of the ZnO NWs synthesized using the MMASD approach at different deposition concentrations. It was clearly found that the prepared samples have a distinct hexagonal wurtzite structure and are vertically oriented and tightly packed onto the substrate whereas the surface morphology changes with different molarity. As discussed by Abu ul Hassan et al., microwave heating provides homogeneous heat transfer to the solution mixture for chemical reactions, thereby speeding up the synthesis process which is clearly evident from all the samples of ZnO NWs produced within a rapid deposition time of 60 minutes [47]. It can also be clearly seen that ZnO NWs at 12.5 mM and 25 mM are more uniformly distributed with even sizes of nanowires as compared to ZnO NWs at 6.25 mM concentration. At higher molarities of 50 mM and 75 mM, however, the wires start fusing with each other and are noticeably greater in diameter size at higher concentrations, and the alkalinity is increased. This can be explained whereby the growth mechanism being boosted by the rise in alkalinity. As the pH of the precursor solution rises due to the increasing concentration, it promotes crystal formation which results in the particle size growing larger as the concentration of the solution increases [48]. Measurements were averaged from individual nanowires in accordance with every sample's area distribution of nanowires, determined using Image J software (Version 1.53t) where the average diameter size of the nanowires is shown in **Table 1.**

The structure of the ZnO NWs samples is affected by variations in the molarity of the deposition solution, and the Zn ion concentration impacts the nucleation process and development of structures affecting the samples' form, size, and density [49-50]. The ZnO sample prepared at the lowest concentration of 6.25 mM has the smallest crystallite size of 23.43 nm and starts increasing at 12.5 mM with 41.28 nm crystallite size. It then continues to grow with the highest crystallite size of 62.80 nm at 25 mM solution concentration. However, it can be noted that although the intensity of the XRD peaks at (002) alignment increases from 25 mM and higher which can be attributed to the nearly perfect alignment of the nanowires, the crystallite size has decreased at 50, and 75 m M concentration. The possible explanation for this counterintuitive relation is the Ostwald ripening process where in a high molarity solution, the smaller particles can dissolve and contribute ions re-deposited on larger ones, leading to the growth of larger particles at the expense of smaller ones. Thus, small particles decrease in size until they disappear, and large particles grow even larger hence the continuous increase in nanowire diameter size and reduction in the crystallite size of the particles. This shrinking and growing of particles will result in a larger mean diameter of a particle size distribution (PSD) [51].

Figure 3 shows The X-ray diffraction (XRD) spectra of the ZnO NWs produced by MMASD method at different deposition solution concentrations. The indexing of the various XRD peaks was carried out in accordance with the Joint Committee on Powder Diffraction Standards (JCPDS) standard database of ZnO hexagonal structure (File No 36-1451). The ZnO NWs produced from all samples are highly crystalline having hexagonal wurtzite structure with preferable c-axis orientation as well as exhibiting seven clear diffraction peaks recorded between 20^o to 70^o. These peaks were indexed at (100), (101), and (002) with the highest intensity and lower at (102), (110), (103), and (112) planes. The samples show a clear and similar trend in the increase of crystallite size with higher molarity in line with the diameter size calculated in **Table 1** with the exception of samples of 50 mM and 75 mM whereby the crystallite size has slightly decreased with increasing diameter size of ZnO NWs. Observations from all the grown samples demonstrate that the particles preferentially evolved in one direction, producing structures that are virtually 1D or rod-like, with the strongest (002) orientation peak, which is seen in all samples, between 33.86 and 33.94°. Contrarily, a few misaligned ZnO NWs grown on the glass substrate may be held accountable for the lower intensities of the other peaks. Generally, the developed samples only showed distinct crystalline structures; no other phase forms, such as amorphous structures, were seen. Additionally, observation shows that the intensity of the XRD peak at (002) alignment increases as the concentration

increases which can be attributed to the nearly perfect alignment of the nanowires.

Moreover, the higher molarity of solutions provides more building blocks (atoms, ions, or molecules) for crystal growth which leads to the formation of larger, more well-defined crystals with fewer defects therefore producing higher crystalline materials with more intense XRD peaks as compared to amorphous or poorly crystalline materials [52]. A higher molarity solution could also lead to a higher particle density on the substrate causing a denser arrangement of particles on the substrate and resulting in more scattering centers for X-rays, leading to increased intensity of the diffracted peaks in the XRD pattern which can also be seen in **Figure 3** [53].

3.2. Optical properties

The optical properties of the generated ZnO NWs are evaluated using UV-VIS spectrometer measurements between 200 and 1200 nm at room temperature. There is a migration of the absorption band edge towards the visible region and a dependence on the precursor in the optical absorption spectra of all synthesized ZnO samples in the visible and ultraviolet ranges. **Figure 4** shows the transmittance spectra of the ZnO NWs made using the MMASD technique at various deposition solution concentrations. The transmittance spectra in the whole visible area display an exciton peak in the 350–380 nm range and decreased absorbance above 380 nm. Strong absorbance in the UV spectrum indicates high crystallinity, whereas sharp absorption edges suggest smaller ZnO particle sizes [54]. The optical transmittance is calculated within the wavelength from 400 and 800 nm and tabulated in **Table 2** where the highest transmittance of 94.24% was recorded for the sample deposited at 12.5 mM concentration. Whereas the sample at 6.25 mM solution concentration recorded the lowest average transmittance of 60.73% over the same wavelength.

Relatively, at the lowest concentration of 6.25 mM solution, the amount of zinc and oxygen ions that are accessible for nucleation is constrained. Thus, resulting in fewer nucleation sites on the substrate. This shortage of nucleation sites can lead to an irregular and sparse distribution of ZnO nanoparticles, resulting in a non-uniform distribution of ZnO film. Hence, several factors could contribute to the decrease in transmittance at lower concentrations of solution. One of them would be due to light scattering whereby as light passes through the thin film, it interacts with the non-uniform surface, leading to the scattering of lights in different directions, and since scattered light does not transmit through the film, the overall transmittance would be reduced. Another factor could be attributed to the surface roughness of the thin film caused by the non-uniformity of ZnO nanowires distribution. When light encounters a rough surface, it undergoes multiple reflections and refractions, as well as diffuse reflection, reducing the amount of transmitted light. However, there is also a decreasing trend of transmittance at higher molarity concentrations specifically at 25, 50, and 75 mM. This could be likely due to the disorganized structures and sizes of ZnO nanowires as seen from the surface image in **Fig 2(d)** and **(e)**. The effect of poorly aligned nanowires on the substrate on light scattering from the surface was also discussed by Tugral et al. Whereas molarity increased, larger diameter nanowires and a less dense nanowire formation on the surface were produced, which increased light scattering and decreased optical transmittance. [55]. Therefore, it is fair to assume that 12.5 mM of solution concentration would be the appropriate concentration of deposition solution to obtain a high enough transmittance of synthesized ZnO NWs for this study.

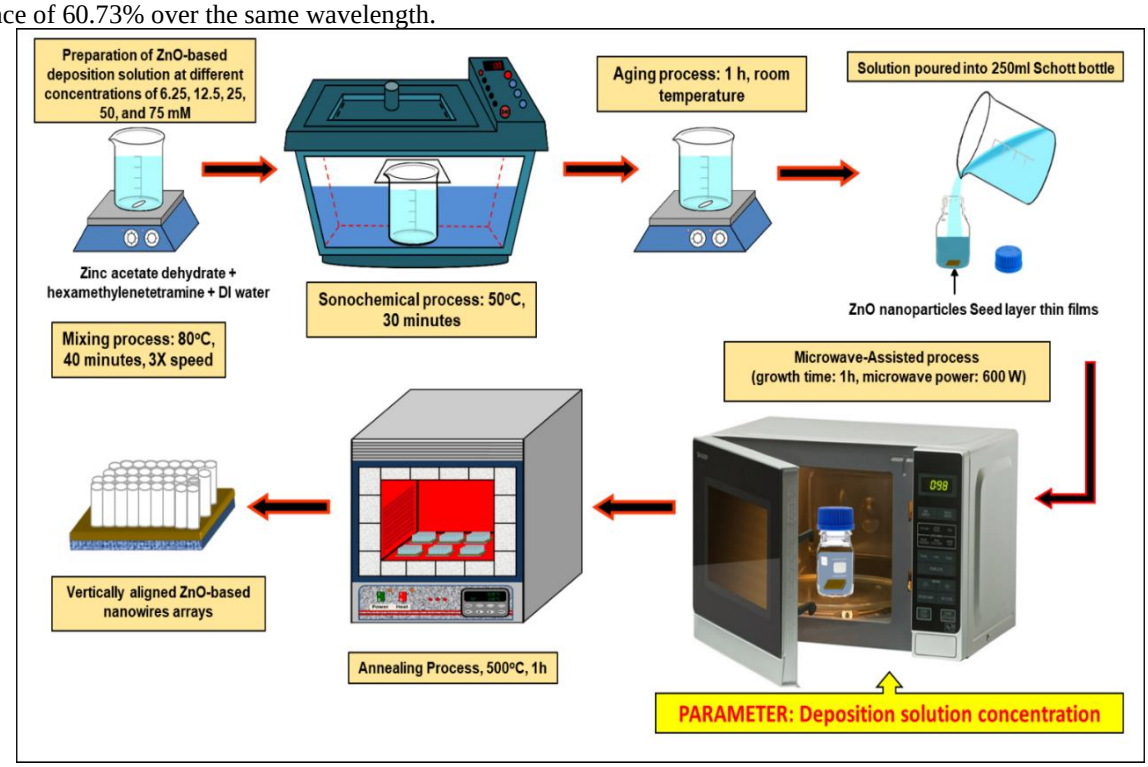

Fig. 1. Schematic diagram on the deposition of ZnO NWs via MMASD method at various deposition solution concentrations.

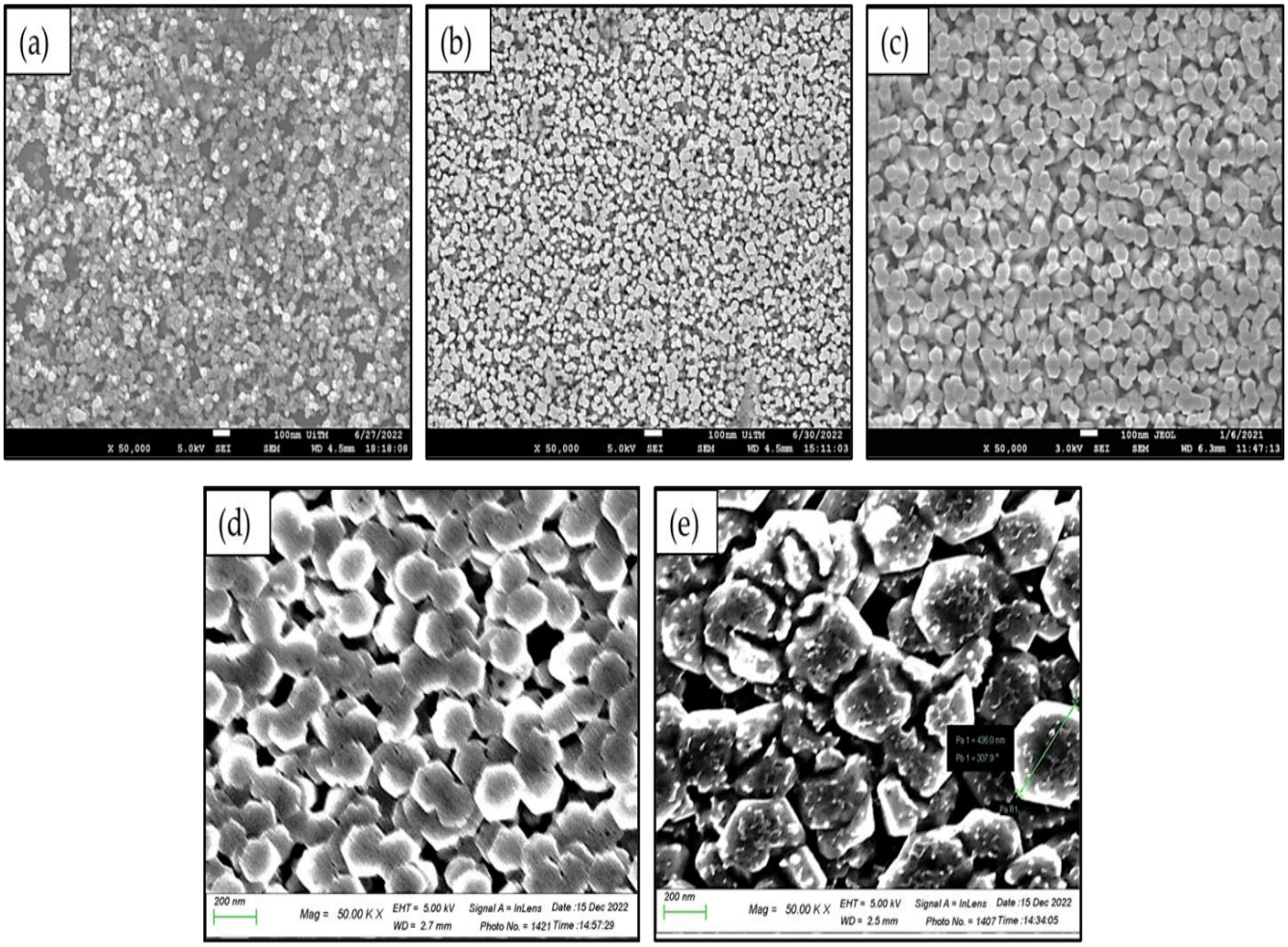

Fig. 2. FESEM images (50k magnification) of ZnO NWs by MMASD method at different molarity of (a) 6.25 mM, (b) 12.5 mM, (c) 25 mM, (d) 50 mM and (e) 75 mM

Table 1: Structural Parameters of ZnO NWs by MMASD method at (a) 6.25 mM, (b) 12.5 mM, (c) 25 mM. (d) 50 mM and (e) 75 mM deposition solution concentration.

Sample	Molarity (mM)	Peak position (2θ)	FWHM (degree, ^{o})	Crystallite size (nm)	FESEM Diameter size (nm)
(a)	6.25	33.86	0.370	23.43	29.49
(b)	12.5	33.94	0.210	41.28	40.61
(c)	25	33.86	0.138	62.80	76.92
(d)	50	33.89	0.171	50.68	209.20
(e)	75	33.86	0.157	55.20	538.11

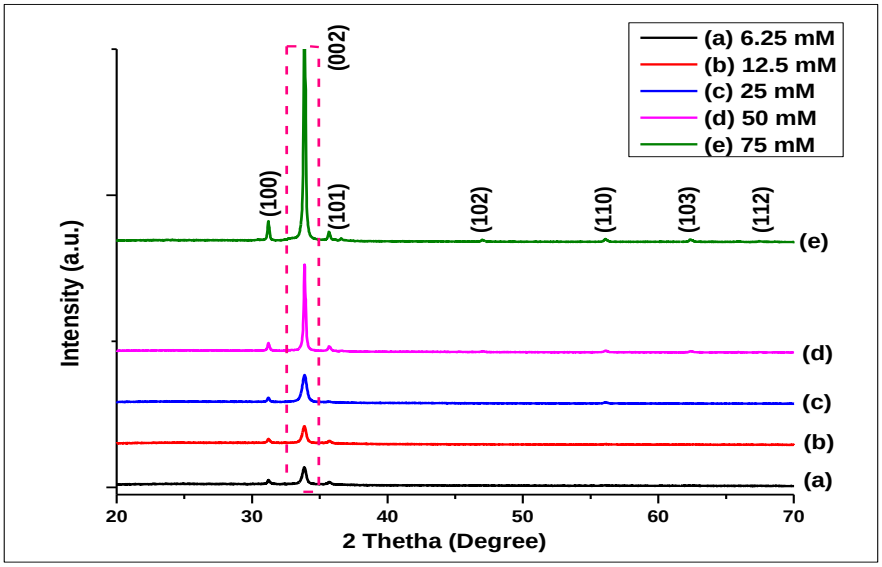

Fig. 3. XRD spectra of ZnO NWs by MMASD method at different molarity of (a) 6.25 mM, (b) 12.5 mM, (c) 25 mM, (d) 50 mM, and (e) 75 mM

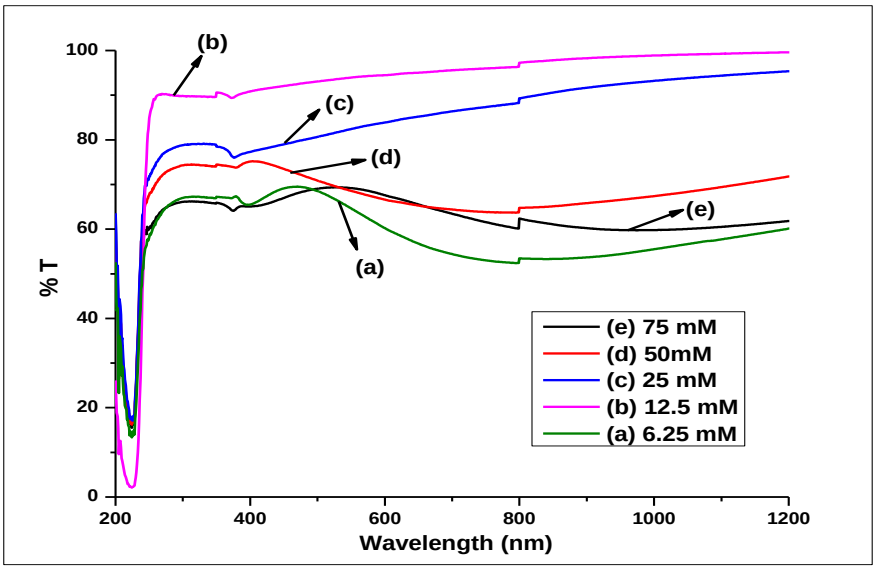

Fig. 4. UV-VIS transmittance spectra of ZnO NWs by MMASD method at different molarity of (a) 6.25 mM, (b) 12.5 mM, (c) 25 mM, (d) 50 mM and (e) 75 mM

Table 2: Average transmittance percentage of ZnO NWs by MMASD at various deposition solution concentrations.

Sample	Molarity (mM)	Average Transmittance (%)
(a)	6.25	60.73
(b)	12.5	94.24
(c)	25	83.47
(d)	50	67.82
(e)	75	65.76

4. Conclusions

In conclusion, highly crystalline ZnO NWs with a hexagonal wurtzite structure and a preferred c-axis orientation were successfully synthesized using a novel modified microwave-assisted sonochemical deposition method at an optimized microwave power of 600 W and rapid deposition time of 60 minutes with the variable of deposition solution concentration. Structural properties found that the peak intensities of the ZnO NWs increase as the molarity increases up to 75 mM indicating highly crystalline ZnO NWs produced. The trend in the growth of the aligned ZnO NWs arrays produced is supported by the FESEM images of samples which indicate an increase in diameter sizes of wires dependent on the concentration of deposition solution with the smallest diameter and most uniform distribution of samples on the substrate at an optimum molarity 12.5 mM. The optical analysis of the samples also found that ZnO NWs obtained by this method have the highest average transmittance of 94.24% for the same 12.5 mM concentration and decrease below and above said molarity. Therefore, the best molarity of deposition solution for the MMASD method would be at 12.5 mM as it produces dense uniformly aligned ZnO nanowires with small diameter and crystallite size as well as high crystallinity with the highest transmittance.

Acknowledgement

This work was supported by Grant No. 600-RMC/GPM COE 5/3 (106/2022) under the Ministry of Higher Education (MOHE) and the Universiti Teknologi MARA (UiTM), Malaysia. The authors would like to thank Ms. Irmaizatussyehdany Buniyamin (Senior Research Officer), Mr. Muhammad Faizal Abd Halim (Assistant Research Officer), Mr. Salifairus Mohammad Jafar (UiTM Senior Science Officer) and Mr. Mohd Azlan Jaafar (UiTM Assistant Engineer) for their kind help and support of this research. All authors declare that they have no conflicts of interest.

References

[1] Z. L. Wang. (2004). Zinc oxide nanostructures: growth, properties and applications. Journal of physics: condensed matter. 16 (25): R829.

[2] J. Zhou, N. S. Xu, and Z. L. Wang. (2006). Dissolving behavior and stability of ZnO wires in biofluids: a study on biodegradability and biocompatibility of ZnO nanostructures. Advanced Materials. 18 (18): 2432-2435.

[3] M. T. Noman, N. Amor, & M. Petru. (2022). Synthesis and applications of ZnO nanostructures (ZONSs): A review. Critical Reviews in Solid State and Materials Sciences. 47 (2): 99-141.

[4] P. Rong, S. Ren, & Q. Yu. (2019). Fabrications and applications of ZnO nanomaterials in flexible functional devices-a review. Critical reviews in analytical chemistry. 49 (4): 336-349.

[5] J. Theerthagiri, S. Salla, R. A. Senthil, P. Nithyadharseni, A. Madankumar, P. Arunachalam, ... & H. S. Kim. (2019). A review on ZnO nanostructured materials: energy, environmental and biological applications. Nanotechnology. 30 (39): 392001.

[6] A. A. Ghassan, N. A. Mijan, & Y. H. Taufiq-Yap. (2019). Nanomaterials: an overview of nanorods synthesis and optimization. Nanorods and nanocomposites. 11 (11): 8-33.

[7] M. S. Lv, C. Li, Y. N. Li, X. F. Zhang, Z. P. Deng, X. L. Cheng, ... & S. Gao. (2023). Facilely controlled synthesis of porous ZnO nanotubes with rich oxygen vacancies for highly sensitive and selective detection of NO2 at low temperature. Sensors and Actuators B: Chemical. 375: 132865.

[8] M. Hong, J. Meng, H. Yu, J. Du, Y. Ou, Q. Liao, ... & Y. Zhang. (2021). Ultra-stable ZnO nanobelts in electrochemical environments. Materials Chemistry Frontiers. 5 (1): 430-437.

[9] A. Galdámez-Martinez, G. Santana, F. Güell, P. R. Martínez-Alanis, & A. Dutt. (2020). Photoluminescence of ZnO nanowires: a review. Nanomaterials. 10 (5): 857.

[10] C. V. Manzano, L. Philippe, & A. Serrà. (2022). Recent progress in the electrochemical deposition of ZnO nanowires: Synthesis approaches and applications. Critical Reviews in Solid State and Materials Sciences. 47 (5): 772-805.

[11] R. Mardosaite, A. Jurkeviciute, & S. Rackauskas. (2021). Superhydrophobic ZnO nanowires: Wettability mechanisms and functional applications. Crystal Growth & Design. 21 (8): 4765-4779.

[12] Y. Zhang, M. K. Ram, E. K. Stefanakos, & D. Y. Goswami. (2012). Synthesis, characterization, and applications of ZnO nanowires. Journal of Nanomaterials. 2012: 1-22.

[13] S. Baruah, R. F. Rafique, & J. Dutta. (2008). Visible light photocatalysis by tailoring crystal defects in zinc oxide nanostructures. Nano. 3 (05): 399-407.

[14] Q. Zhou, J. Z. Wen, P. Zhao, & W. A. Anderson. (2017). Synthesis of vertically-aligned zinc oxide nanowires and their application as a photocatalyst. Nanomaterials. 7 (1): 9.

[15] Ü. Özgür, Y. I. Alivov, C. Liu, A. Teke, M. A. Reshchikov, S. Doğan, ... & A. H. Morkoç. (2005). A comprehensive review of ZnO materials and devices. Journal of applied physics. 98 (4).

[16] A. Moezzi, A. M. McDonagh, & M. B. Cortie. (2012). Zinc oxide particles: Synthesis, properties and applications. Chemical engineering journal. 185: 1-22.

[17] F. H. Abdullah, N. A. Bakar, & M. A. Bakar. (2022). Current advancements on the fabrication, modification, and industrial application of zinc oxide as photocatalyst in the removal of organic and inorganic contaminants in aquatic systems. Journal of hazardous materials. 424: 127416.

[18] H. O. Chu, W. A. N. G. Quan, Y. J. Shi, S. G. Song, W. G. Liu, Z. H. O. U. Shun, ... & L. I. Cheng. (2020). Structural, optical properties and optical modelling of hydrothermal chemical growth derived ZnO nanowires. Transactions of Nonferrous Metals Society of China. 30 (1): 191-199.

[19] M. A. Messih, M. A. Ahmed, A. Soltan, & S. S. Anis. (2019). Synthesis and characterization of novel Ag/ZnO nanoparticles for photocatalytic

degradation of methylene blue under UV and solar irradiation. Journal of Physics and Chemistry of Solids. 135: 109086.

[20] T. Van Khai, V. M. Thanh, & T. Dai Lam. (2018). Structural, optical and gas sensing properties of vertically well-aligned ZnO nanowires grown on graphene/Si substrate by thermal evaporation method. Materials Characterization. 141: 296-317.

[21] H. Ahmoum, G. Li, S. Belakry, M. Boughrara, M. S. Su'ait, M. Kerouad, & Q. Wang. (2021). Structural, morphological and transport properties of Ni doped ZnO thin films deposited by thermal co-evaporation method. Materials Science in Semiconductor Processing. 123: 105530.

[22] P. Narin, E. Kutlu-Narin, S. Kayral, R. Tulek, S. Gokden, A. Teke, & S. B. Lisesivdin. (2022). Morphological and optical characterizations of different ZnO nanostructures grown by mist-CVD. Journal of Luminescence. 251: 119158.

[23] M. Bai, M. Chen, X. Li, & Q. Wang. (2022). One-step CVD growth of ZnO nanorod/SnO2 film heterojunction for NO2 gas sensor. Sensors and Actuators B: Chemical. 373: 132738.

[24] R. Ebrahimifard, H. Abdizadeh, & M. R. Golobostanfard. (2020). Controlling the extremely preferred orientation texturing of sol–gel derived ZnO thin films with sol and heat treatment parameters. Journal of Sol-Gel Science and Technology. 93: 28-35.

[25] T. Amakali, L. Daniel, V. Uahengo, N. Y. Dzade, & N. H. De Leeuw. (2020). Structural and optical properties of ZnO thin films prepared by molecular precursor and sol–gel methods. Crystals. 10 (2): 132.

[26] C. V. Manzano, L. Philippe, & A. Serrà. (2022). Recent progress in the electrochemical deposition of ZnO nanowires: Synthesis approaches and applications. Critical Reviews in Solid State and Materials Sciences. 47 (5): 772-805.

[27] G. Zou, H. Li, Y. Zhang, K. Xiong, & Y. Qian. (2006). Solvothermal/hydrothermal route to semiconductor nanowires. Nanotechnology. 17 (11): S313.

[28] S. Zhao, Y. Shen, X. Yan, P. Zhou, Y. Yin, R. Lu, ... & D. Wei. (2019). Complex-surfactant-assisted hydrothermal synthesis of one-dimensional ZnO nanorods for high-performance ethanol gas sensor. Sensors and Actuators B: Chemical. 286: 501-511.

[29] P. Basnet, & S. Chatterjee. (2020). Structure-directing property and growth mechanism induced by capping agents in nanostructured ZnO during hydrothermal synthesis—A systematic review. Nano-Structures & Nano-Objects. 22: 100426.

[30] M. N. I. Ghazali, M. A. Izmi, S. N. A. Mustaffa, S. Abubakar, M. Husham, S. Sagadevan, & S. Paiman. (2021). A comparative approach on One-Dimensional ZnO nanowires for morphological and structural properties. Journal of Crystal Growth. 558: 125997.

[31] P. Saravanan, K. SenthilKannan, M. Vimalan, S. Tamilselvan, & D. Sankar. (2020). Biofriendly and competent domestic microwave assisted method for the synthesis of ZnO nanoparticles from the extract of Azadirachta indica leaves. Materials Today: Proceedings. 33: 3160-3163.

[32] C. Mallikarjunaswamy, V. L. Ranganatha, R. Ramu, Udayabhanu, & G. Nagaraju. (2020). Facile microwave-assisted green synthesis of ZnO nanoparticles: application to photodegradation, antibacterial and antioxidant. Journal of Materials Science: Materials in Electronics. 31: 1004-1021.

[33] P. P. Ortega, C. C. Silva, M. A. Ramirez, G. Biasotto, C. R. Foschini, & A. Z. Simoes. (2021). Multifunctional environmental applications of ZnO nanostructures synthesized by the microwave-assisted hydrothermal technique. Applied Surface Science. 542: 148723.

[34] A. Kumar, Y. Kuang, Z. Liang, & X. Sun. (2020). Microwave chemistry, recent advancements, and eco-friendly microwave-assisted synthesis of nanoarchitectures and their applications: A review. Materials Today Nano. 11: 100076.

[35] C. Mallikarjunaswamy, V. Lakshmi Ranganatha, R. Ramu, Udayabhanu, & G. Nagaraju. (2020). Facile microwave-assisted green synthesis of ZnO nanoparticles: application to photodegradation, antibacterial and antioxidant. Journal of Materials Science: Materials in Electronics. 31: 1004-1021.

[36] N. Devi, S. Sahoo, R. Kumar, & R. K. Singh. (2021). A review of the microwave-assisted synthesis of carbon nanomaterials, metal oxides/hydroxides and their composites for energy storage applications. Nanoscale. 13 (27): 11679-11711.

[37] N. Garino, T. Limongi, B. Dumontel, M. Canta, L. Racca, M. Laurenti, ... & V. Cauda. (2019). A microwave-assisted synthesis of zinc oxide nanocrystals finely tuned for biological applications. Nanomaterials. 9 (2): 212.

[38] K. J. Rao, B. Vaidhyanathan, M. Ganguli, & P. A. Ramakrishnan. (1999). Synthesis of inorganic solids using microwaves. Chemistry of materials. 11 (4): 882-895.

[39] B. D. Cullity. (1956). Elements of X-ray Diffraction. Addison-Wesley Publishing.

[40] H. M. Kingston and S. J. Haswell. (1997). Overview of microwave-assisted sample preparation. Microwave Enhanced Chemistry: Fundamentals, Sample Preparation and Applications. American Chemical Society, Washington DC. 55-222.

[41] Y. He. (2004). Synthesis of ZnO nanoparticles with narrow size distribution under pulsed microwave heating. China Particuology. 2 (4): 168-170.

[42] O. Palchik, J. Zhu, & A. Gedanken. (2000). Microwave assisted preparation of binary oxide nanoparticles. Journal of Materials Chemistry. 10 (5): 1251-1254.

[43] S. Horikoshi, R. F. Schiffmann, J. Fukushima, & N. Serpone. (2018). Microwave chemical and materials processing. In Microwave Chemical and Materials Processing (pp. 33-45). Springer Singapore, Singapore.

[44] M. H. Mamat, M. Z. Sahdan, Z. Khusaimi, A. Z. Ahmed, S. Abdullah, & M. Rusop. (2010). Influence of doping concentrations on the aluminum doped zinc oxide thin films properties for ultraviolet photoconductive sensor applications. Optical materials. 32 (6): 696-699.

[45] M. F. Malek, M. H. Mamat, M. Z. Musa, T. Soga, S. A. Rahman, S. A. Alrokayan, ... & M. Rusop. (2015). Metamorphosis of strain/stress on optical band gap energy of ZAO thin films via manipulation of thermal annealing process. Journal of Luminescence. 160: 165-175.

[46] X. Ge, K. Hong, J. Zhang, L. Liu, & M. Xu. (2015). A controllable microwave-assisted hydrothermal method to synthesize ZnO nanowire arrays as recyclable photocatalyst. Materials Letters. 139: 119-121.

[47] A. U. H. S. Rana, & H. S. Kim. (2018). Growth condition-oriented defect engineering for changes in Au–ZnO contact behavior from Schottky to Ohmic and vice versa. Nanomaterials. 8 (12): 980.

[48] S. V. Elangovan, V. Chandramohan, N. Sivakumar, & T. S. Senthil. (2016). Synthesis and characterization of ZnO nanoparticles at different molarity concentrations for photocatalytic applications. Desalination and water treatment. 57 (21): 9671-9678.

[49] R. Rayathulhan, B. K. Sodipo, & A. A. Aziz. (2017). Nucleation and growth of zinc oxide nanorods directly on metal wire by sonochemical method. Ultrasonics sonochemistry. 35: 270-275.

[50] M. Soylu, & M. J. J. O. A. Coskun. (2018). Controlling the properties of ZnO thin films by varying precursor concentration. Journal of Alloys and Compounds. 741: 957-968.

[51] H. J. Lee, U. J. Yang, K. N. Kim, S. Park, K. H. Kil, J. S. Kim, ... & J. M. Baik. (2019). Directional Ostwald ripening for producing aligned arrays of nanowires. Nano letters. 19 (7): 4306-4313.

[52] J. Fang, B. Ding, & H. Gleiter. (2011). Mesocrystals: Syntheses in metals and applications. Chemical Society Reviews. 40 (11): 5347-5360.

[53] S. Joishy, S. D. Kulkarni, R. J. Choudary, S. R. Maidur, P. S. Patil, & B. V. Rajendra. (2019). Influence of solution molarity on structure, surface morphology, non-linear optical and electric properties of CdO thin films prepared by spray pyrolysis technique. Materials Research Express. 6 (10): 106447.

[54] K. P. Sridevi, S. Sivakumar, & K. Saravanan. (2021). Synthesis and Characterizations of Zinc Oxide Nanoparticles Using Various Precursors. Annals of the Romanian Society for Cell Biology. 8679-8689.

[55] H. T. Arslan, C. Arslan, & N. Baydogan. (2022). The effects of the curing parameters of the hydrothermal solution on the characteristic properties of ZnO nanowires. Journal of Optics. 51 (1): 79-88.